C. H. Kruger, Principal Investigator
C. O. Laux, Associate Investigator

Mechanical Engineering Department
Stanford University
Stanford, California 94305

Contents

1. Introduction

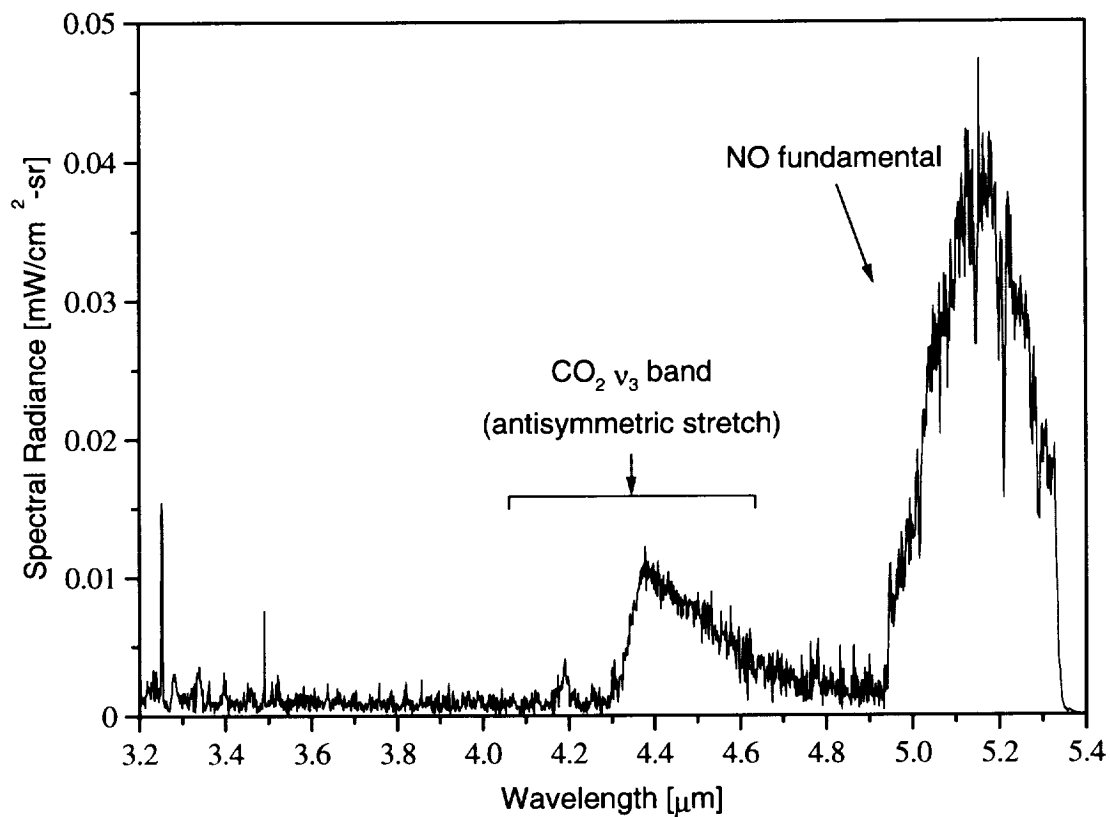This report describes progress during the second year of our research program on Infrared Signature Masking by Air Plasmas at Stanford University. This program is intended to investigate the masking of infrared signatures by the air plasma formed behind the bow shock of high velocity missiles. This research is currently directed by Professor Charles H. Kruger, with Dr. Christophe O. Laux as associate investigator. This program is supported by a grant from the Ballistic Missile Defense Organization (technical monitor: Dr. David Mann) and is currently funded through the National Aeronautics and Space Administration (NAG 2-1079) with Dr. Stephanie R. Langhoff from NASA-Ames as technical monitor. One Ph.D. candidate is currently involved in this program.

Our previous annual report described spectral measurements and modeling of the radiation emitted between 3.2 and 5.5 μm by an atmospheric pressure air plasma in chemical and thermal equilibrium at a temperature of approximately 3100 K. One of our goals was to examine the spectral emission of secondary species such as water vapor or carbon dioxide. The cold air stream injected in the plasma torch contained approximately 330 parts per million of CO_2, which is the natural CO_2 concentration in atmospheric air at room temperature, and a small amount of water vapor with an estimated mole fraction of 3.8×10^{-4}. As can be seen from Figure 1, it was found that the measured spectrum exhibited intense spectral features due to the fundamental rovibrational bands of NO at 4.9-5.5 μm and the v_3 band of CO_2 (antisymmetric stretch) at 4.2-4.8 μm. These observations confirmed the well-known fact that infrared signatures between 4.15 –5.5 μm can be masked by radiative emission in the interceptor's bow-shock.

Figure 1 also suggested that the range 3.2 – 4.15 μm did not contain any significant emission features (lines or continuum) that could mask IR signatures. However, the signal-to-noise level, close to one in that range, precluded definite conclusions. Thus, in an effort to further investigate the spectral emission in the range of interest to signature masking problem, new measurements were made with a higher signal-to-noise ratio and an extended wavelength range.

Figure 1. Measured IR emission spectrum of ~3100 K, atmospheric pressure air (see 1996-1997 annual report).

2. Experiment

2.1. Experimental setup and conditions

A full description of the experimental facility was given in the 1996-1997 Annual Report. For the measurements presented in this report, experimental conditions were essentially the same as in our previous work with the following difference. First, slightly wider monochromator slits were employed to improve the signal to noise ratio (the entrance and exit slits were set at 1.0 and 2.8 μm, respectively, vs. 0.75 and 2.8 μm previously). Second, a larger amount of H_2O was injected in the torch (4.5×10^{-3} vs. 3.8×10^{-4} H_2O mole fraction) as OH fundamental bands are expected to radiate at wavelengths between 2.5 and 4.15 μm. Third, the spectral range was extended to cover 2.4 – 5.5 μm (vs. 3.2–5.5 μm previously) so as to capture NO first overtone and OH fundamental rovibrational bands. The measured temperature profile, shown in Figure 2, was determined as in our earlier work from Abel-inverted profiles of absolute NO (1-0) bandhead intensities. The current temperature profile is approximately 300 K higher than in our earlier experiments (the maximum temperature is now ~3400 K vs. ~3100 K), a difference on the order of experimental uncertainties. For the present conditions, concentration profiles of major radiating species are shown in Figure 2. These concentrations were obtained by assuming chemical equilibrium at atmospheric pressure and at the measured temperatures since, as discussed in our previous annual report, the plasma produced by the torch under the present conditions was found to be close to Local Thermodynamic Equilibrium.
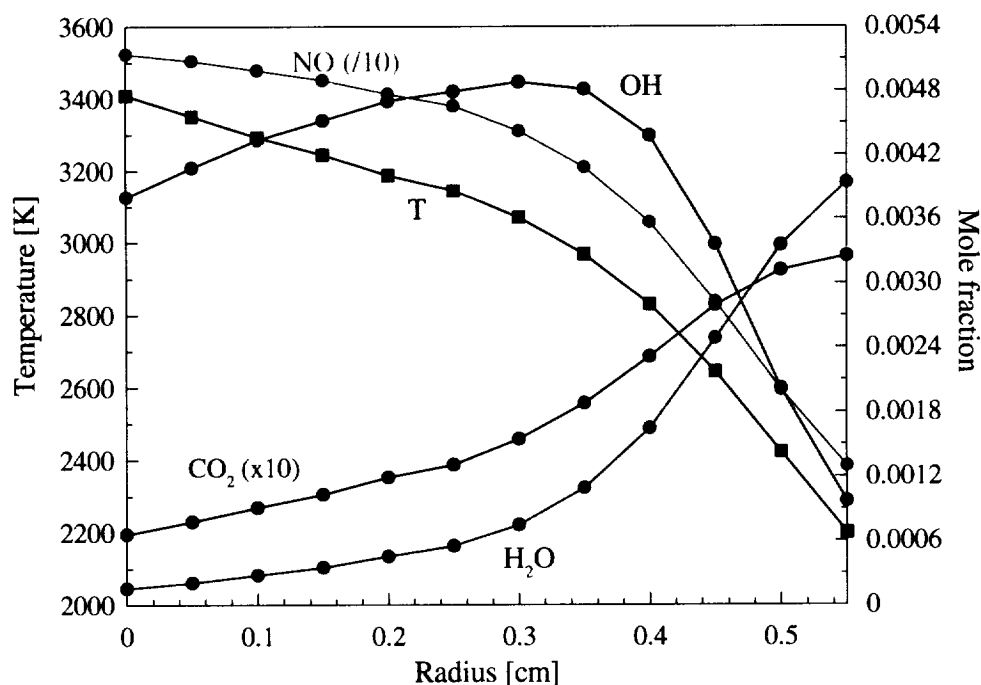

Figure 2. Temperature and concentration profiles (major radiating species) for the conditions of the spectrum presented in Figure 3 and subsequent figures of the present report.

2.2. Spectral Calibration Procedure

As in our earlier experiments, the calibration was conducted using a radiance standard (Optronics Laboratories model OL550 tungsten strip) traceable to NIST standards. The calibration procedure is somewhat complicated by absorption features due to the water vapor and carbon dioxide present over the 6-meter optical path that separates the plasma source or calibration lamp from the detector. These two species absorb a significant fraction of emission between 1.5 and 2.9 μm and at wavelengths ≥ 4.0 μm. Both the calibration and the plasma torch emission spectra are affected by room air absorption. It could be thought possible to recover the calibrated plasma torch emission spectrum by simply dividing the measured plasma torch signal by the calibration signal. Such a procedure would be flawed as absorption lines of room air may occur at different wavelengths than plasma emission lines. In other words, the absorption lines observed in the calibration spectrum may not absorb any plasma emission. The correct procedure is to deconvolve room air absorption from the calibration signal, and then to divide the plasma emission signal by the corrected (i.e. room air absorption corrected) calibration signal. With this procedure, the calibrated plasma spectrum represents the spectrum emitted by the plasma and absorbed by room air. Thus the absorption features of water vapor and carbon dioxide remain part of the experimental plasma emission spectrum. In order to model this spectrum, it is then necessary to determine the spectral emission of the plasma and then to solve the transport equation over a path of room air. The deconvolution procedure is presented next.

Deconvolution of room air absorption features from the calibration signal:

The raw calibration signal (PMT voltage) is shown in Figure 3. The absorption features of room air species (CO_2 and H_2O) are indicated. Absorption by CO_2 at 4.3 μm can be removed by a straight line interpolation. This approximation is certainly valid because the OL550 tungsten filament emission and the grating response are smoothly varying in that spectral range. The other absorption features occur over wider wavelength ranges and cannot be deconvolved using such a simple procedure. For these features, our deconvolution procedure consists in dividing the calibration signal by the spectral transmission spectrum (convolved with the instrumental slit function) of room air. The transmission spectrum of room air was obtained with the HITRAN96 database[12] with the following parameters: room temperature of 298 K, path length of 6 meters, water vapor mole fraction of 0.013 and CO_2 mole fraction of 0.001 (1000 ppm).
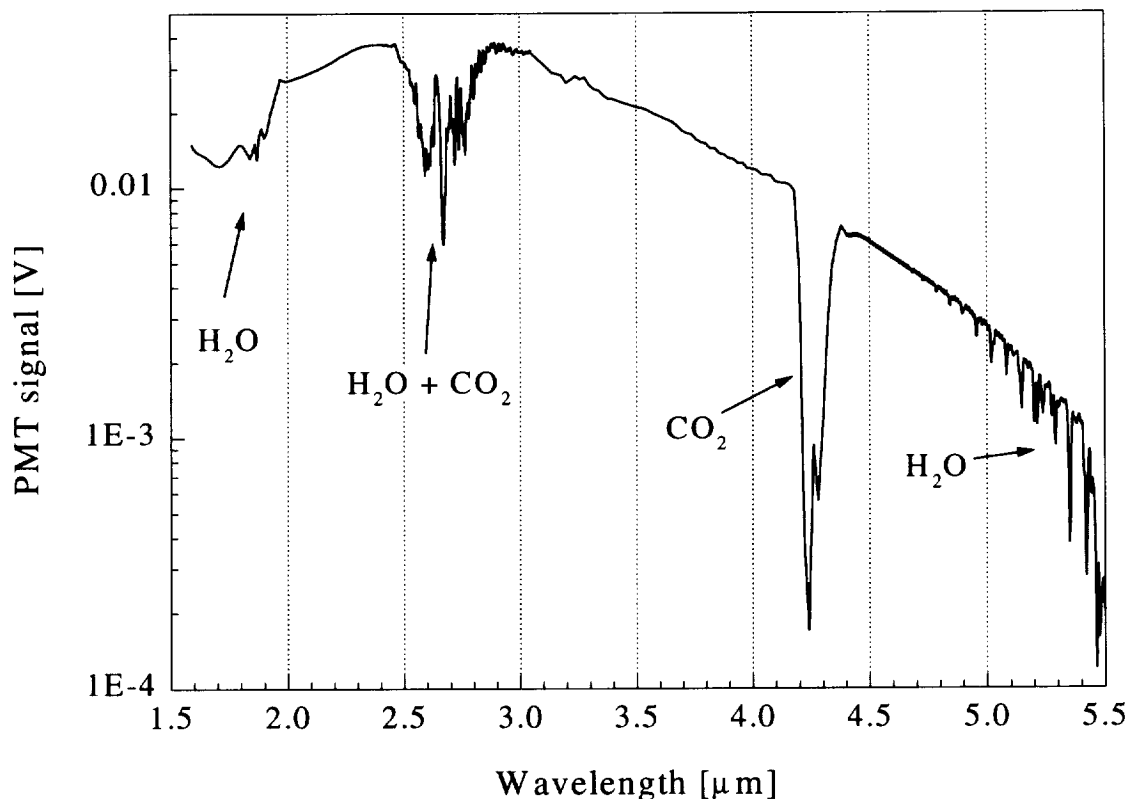
Figure 3. Raw calibration spectrum obtained with the OL550 calibration standard.

Results of the deconvolution procedure around 1.8 and 2.7 μm are presented in Figure 4. The red curve represents the corrected calibration using the absorption coefficient determined with HITRAN. As can be seen in Figure 4, the deconvolution procedure at 1.8 μm produces a smoothly varying trace. At 2.7 μm, the recovered spectrum still shows residual H_2O absorption lines which cannot be removed by varying the H_2O mole fraction. We believe that these residual features could be due to inaccuracies in the HITRAN database or to uncertainties on the instrumental slit-function which was deduced from the entrance and exit slit-width readings and the theoretical reciprocal linear dispersion of the monochromator. In future work, the slit functions will be measured experimentally with a monochromatic light source to increase the accuracy of the deconvolution procedure. The recovered calibration spectrum between 2.5 μm and 3.0 μm shows a cusp and an S-shape variation that is likely due to the spectral response of this ruled grating. Since the grating spectral response should be relatively smooth, we replaced the part of the red curve between 2.5 and 3.0 μm with a fourth order polynomial fit (blue curve).
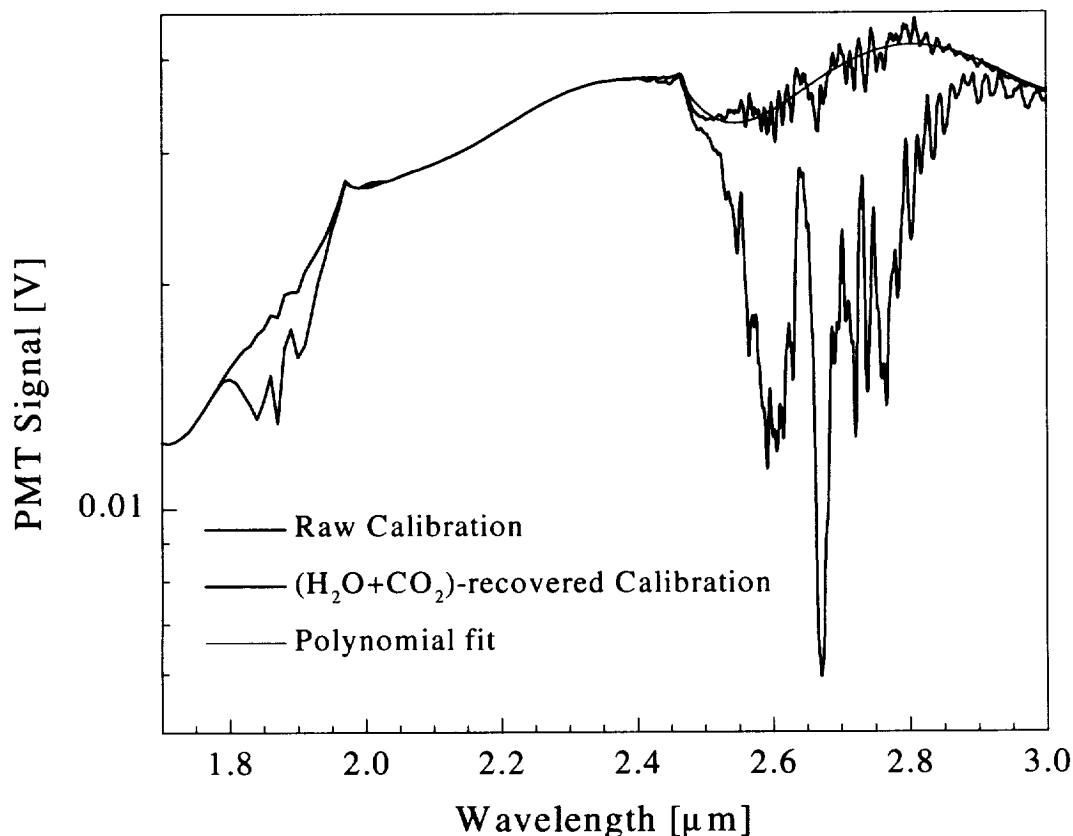
Figure 4. Absorption-deconvolved calibration spectrum in range 1.7-3.0 μm (The absorption features are due to room air H₂O and CO₂).

Results of the deconvolution procedure between 4.5 μm and 5.5 μm are presented in Figure 5. In this range, room air absorption is mostly due to H_2O. As can be seen from the figure, the deconvoluted calibration signal exhibits very smooth variations in this spectral range. The small oscillations are due to an etaloning interference by the quartz window of the OL550 calibration lamp. These oscillations and residual variations due to inaccuracies on the recovery procedure were finally smoothed out using adjacent averaging (blue curve).

Figure 6 shows the summary comparison between the raw calibration spectrum and the deconvolved calibration spectrum.
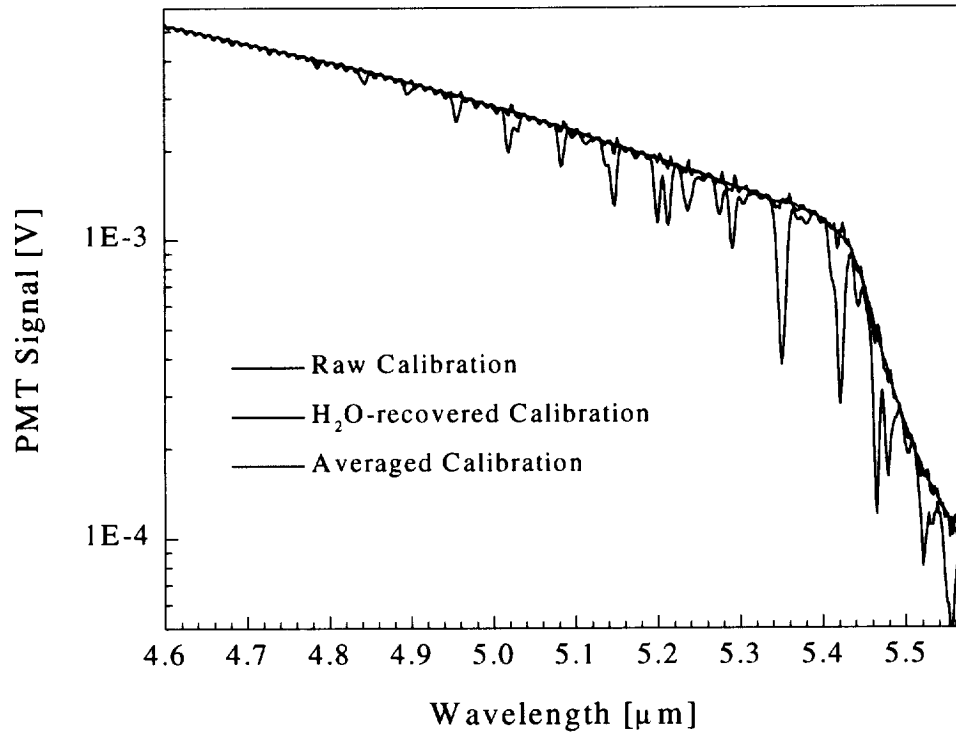
Figure 5. Absorption-deconvolved calibration spectrum in range 4.6-5.6 μm (The absorption features are due to room air H₂O).
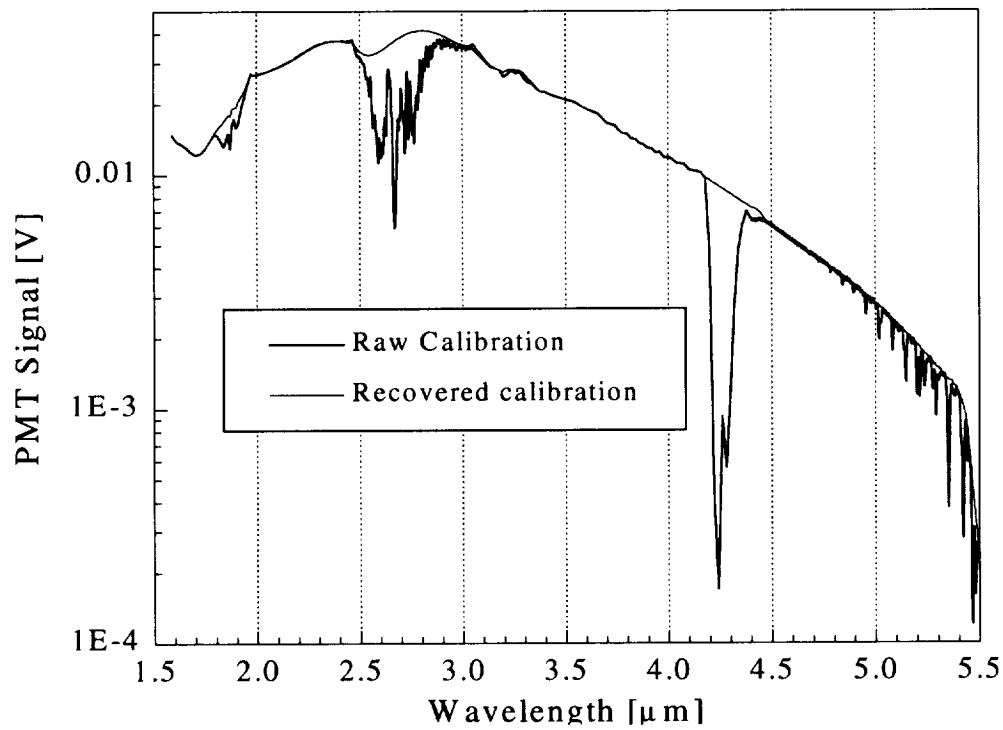

Figure 6. Calibration spectrum corrected for water vapor and carbon dioxide absorption.

9

1. Radiation Model

The measured emission spectrum, corrected for the spectral response of the detection system and calibrated in absolute intensity using the procedure discussed in the foregoing section, is presented in Figure 7. As in our earlier set of experiments, both the fundamental bands of NO at ~5 μm, and the v_3 band of CO_2 at ~4.3 μm are observed. But in addition the region 2.5–4.15 μm exhibits lines of OH fundamental and of the NO first overtone (Δv=2). We summarize next our modeling efforts for these radiative transitions.

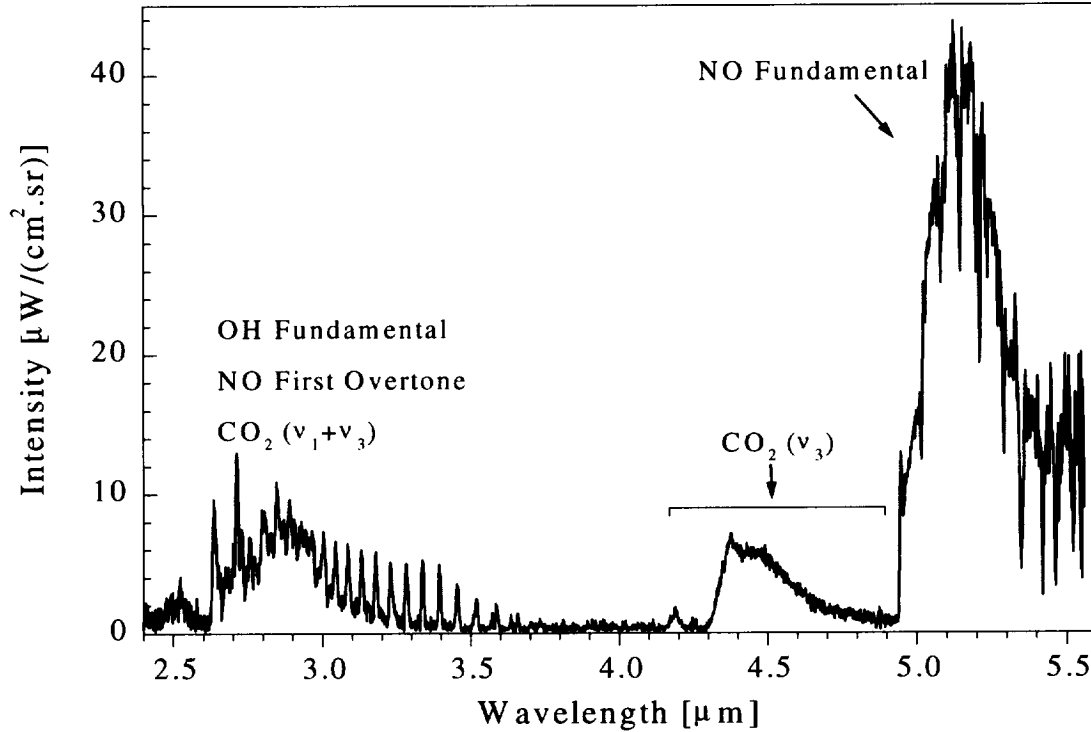Figure 7. Measured IR emission spectrum
(present work: P=1 atm, maximum plasma temperature = ~3400K).

3.1. NO rovibrational bands (fundamental and first overtone)

The fundamental (Δv = 1) and first overtone (Δv = 2) rovibrational bands of NO ($X^2\Pi$) are clearly seen in the experimental spectrum shown in Figure 7. A detailed, accurate model of fundamental and overtone bands of NO ($X^2\Pi$) was implemented in NEQAIR2-IR, as previously described in Ref. [1]. The code determines rotational line positions by diagonalizing the Hamiltonian published by Amiot.[2] For each vibrational band, vibrational dipole moments $M_{v'v''}$ defined as:

$$\left(M_{v'v''}\right)^2 = \left(\int \Psi_{v'}(r)D_e(r)\Psi_{v'}(r)dr\right)^2,$$

where D_e stands for the electric dipole moment function (EDMF), were determined using the accurate *ab initio* EDMF of Langhoff et al.[3] The Hönl-London factor expressions

(corresponding to Hund's case a) recommended by Spencer et al[4] were employed. The model provides very accurate line intensities and spectral positions, which is of particular importance for high-resolution spectroscopic diagnostics and for the accurate simulation of absorption of fundamental and overtone NO bands by atmospheric water vapor.

3.2. CO₂ bands: v_3 antisymmetric stretch at 4.3 μm and (v_1+v_3) band at 2.7 μm

Computations of the CO_2 band spectrum at 2.7 and 4.3 μm were obtained with the *correlated-k* model[5] based on the parameters of EM2C Laboratory of the Ecole Centrale Paris.[6,7] The *correlated-k* model is a narrow-band model in which the actual spectrum is replaced on each narrow band by the reordered spectrum, so that the spectral integration is carried out using typically 10 points instead of several thousands. In the case of CO_2 IR radiation, this model affords radiative intensity predictions within a few percent accuracy.[7] The parameters used for the simulations presented in this report are based on a 16-point Gaussian quadrature and a spectral decomposition over intervals of width 25 cm^{-1}.

3.3. OH rovibrational bands

The fundamental ($\Delta v = 1$) bands of OH ($X^2\Pi$) are clearly seen between 2.5 and 4 μm in the experimental spectrum shown in Figure 7. As for the NO IR bands, an accurate line-by-line model of fundamental (and overtone) bands of OH ($X^2\Pi$) was incorporated in NEQAIR2-IR. Rovibrational term energies and line positions for the 1-0 and 2-1 bands of this transition are determined by diagonalizing the Hamiltonian of Stark *et al.* [8] (with corrections of Levin *et al.* [9]). In future work, we also intend to incorporate additional bands originating in higher vibrational levels, with line positions for these levels determined using the Hamiltonian of Coxon.[10]. Transition probabilities of the OH IR lines have a very strong dependence on centrifugal distortions of the vibrational potentials. As a result, the P and R branches show an anomalous distribution with intense P branches and very weak R branches. In the NEQAIR2-IR model, we utilized the P- and R-branch transition probabilities determined by Holtzclaw et al.[11] As for the case of NO IR bands, this model provides the highly accurate spectral positions required for reliable simulations of absorption by atmospheric water vapor.

3.4. Water vapor absorption

In this work, the HITRAN96 database[12] was used to determine the transmittance spectrum of room air, based on a water mole fraction of 0.014 and a carbon dioxide mole fraction of 0.001 over a 6-meter optical path (for more details, see Section 4.3). The procedure for taking into account absorption is as follows: first, the emission spectrum of the plasma is computed at high spectral resolution (10 points/angstrom, or approximately 10 points per line). Then, attenuation of this spectrum as a result of water vapor and carbon dioxide absorption is determined with Beer's law, using the line strengths and

spectral broadening coefficients of H_2O and CO_2 (HITRAN96 database). Finally, the resulting spectrum is convolved with the instrumental slit function.

4. Comparison of measured and computed spectra

4.1. Range 2.4–4.2 μm

The spectrum measured over the range 2.4–4.2 μm is compared with the spectral predictions of NEQAIR2-IR in Figure 8. As can be seen, all spectral features are well reproduced by the simulations, except perhaps between 2.8 and 3.0 μm where the model slightly underpredicts the measurements (possibly because we have not yet incorporated the (3-2) band of OH in NEQAIR2-IR).

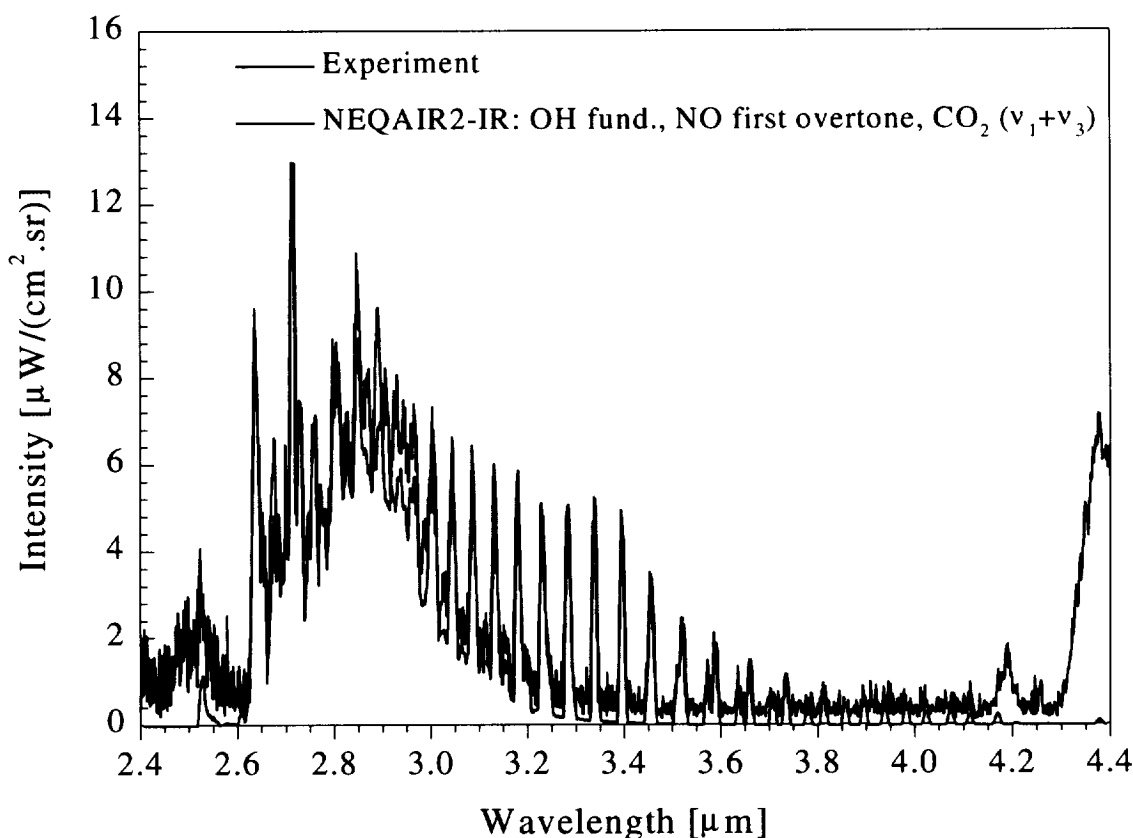**Figure 8. Measured emission spectrum in the range 2.4 – 4.4 μm and comparison with NEQAIR2-IR simulations.**

The contributions of the various radiating systems of importance in this spectral range are shown separately in Figure 9. It can be seen that the P-branch of OH extends into the CO_2 v_3 band at 4.3 μm. Thus, OH emission may pose a problem for the detection of IR signatures in this spectral range.

The mole fraction of OH was determined by matching the measured absolute intensities of rotational lines of the P-branch of OH. The OH concentration determined in this manner was then used to infer, using chemical equilibrium relations, the mole fraction of water in the air injected inside the plasma torch. As already mentioned in the introduction, the mole fraction of water injected in the torch was thus found to be approximately 4.5×10^{-3}. This value is significantly lower than the mole fraction of water vapor in room air (0.013). This difference is not surprising as the air injected in the torch was prepared by compressing atmospheric air at an earlier time when the relative humidity may have been lower, and/or significant amount of water vapor may have been removed by the water trap mounted at the exit compressed air tank The presence of this water trap is unfortunately required for separate experiments that use the same compressed air tank.
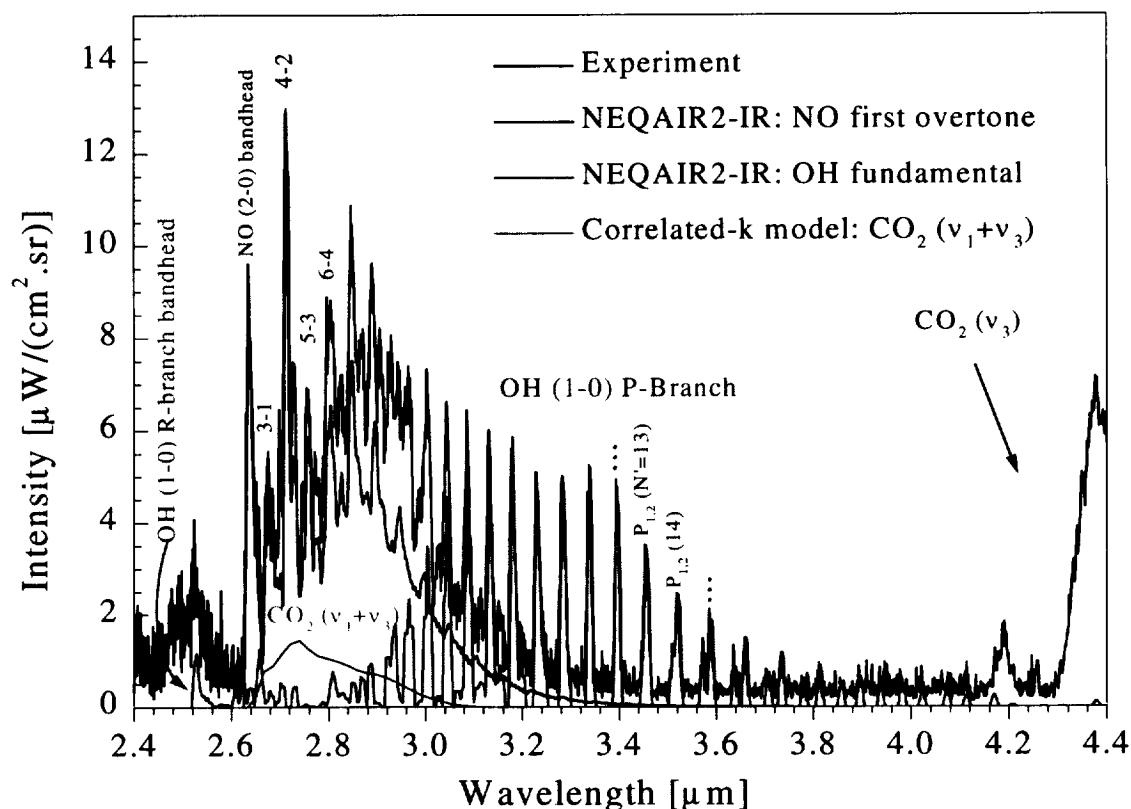

Figure 9. Contributions of NO first overtone, OH fundamental, and CO_2 (v_1+v_3) bands to the total emission spectrum in the range 2.4 – 4.4 μm. Note the anomalously weak OH R branch. These simulations incorporate room air absorption over a 6-meter pathlength.

Absorption by water vapor in the 6 meter optical path is particularly significant between 2.5 and 2.95 μm, as can be seen in Figure 10 where spectral simulations obtained with and without water absorption are compared with the measured spectrum. This comparison underscores the importance of computing highly accurate positions for all emission and absorption spectral lines, in the present case those of the NO overtone, OH fundamental, and H_2O absorption bands.
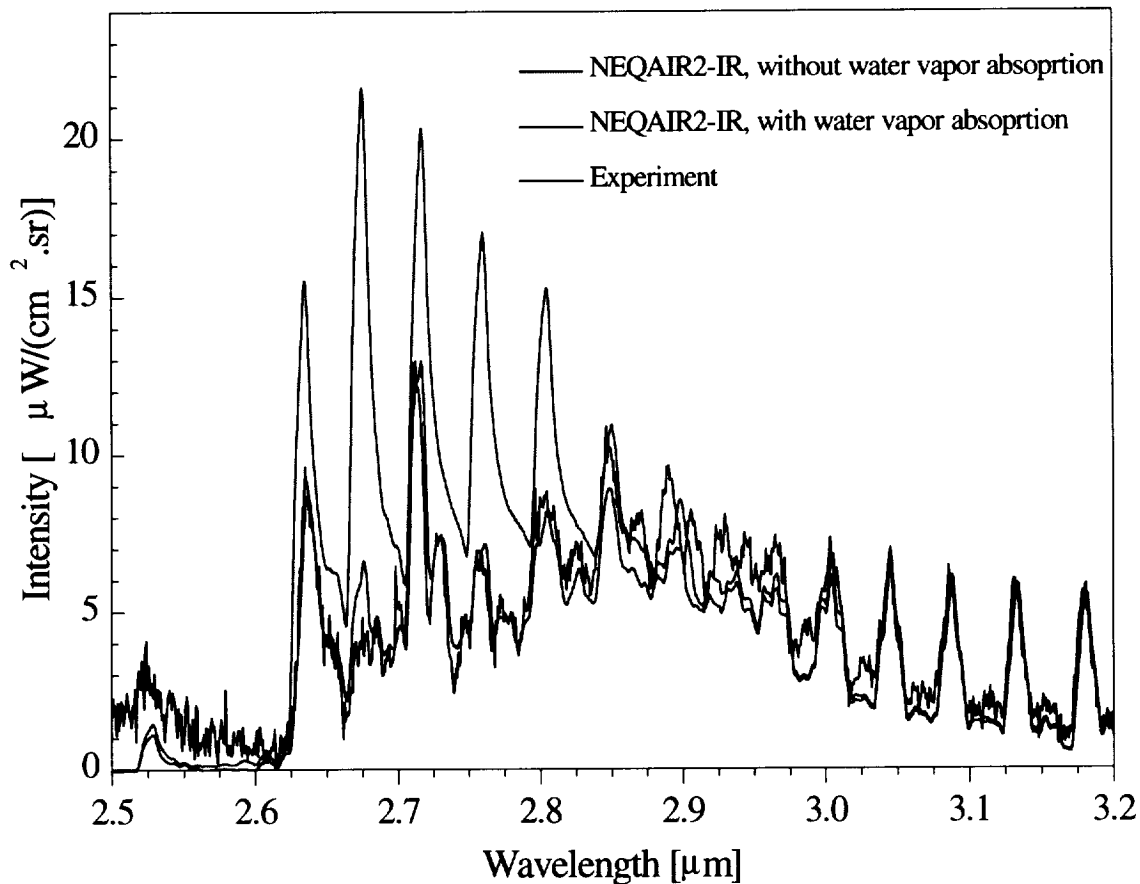
13

Figure 10. Comparison between the measured emission spectrum and NEQAIR2-IR simulations with and without absorption by water vapor in the optical path.

4.2. Range 4.1 – 4.9 μm

Figure 11 compares the measured CO_2 v_3 band spectrum with the predictions of the *correlated-k* model[5] presented in Section 2.2. The model also accounts for absorption by room air CO_2 over the optical path separating the plasma from the detector. This absorption is clearly responsible for near extinction in the range 4.2-4.3 μm of the emission from low-lying rotational levels of CO_2. The lines appearing at both edges of the absorbed region correspond to "hot" CO_2 rotational lines. The model appears to overestimate the measured CO_2 band intensity by approximately 30%. This discrepancy may be due to the fact that the parameters used in the c-k model are only valid at temperatures below 2900 K, which is a temperature slightly lower than the maximum temperature of the plasma considered here (max. temp. = 3400 K). Another possible reason for the discrepancy may be that the air injected in the torch contained a lower concentration of CO_2 than the typical 330 ppm. Excellent agreement between the simulations and the experiment would be obtained by assuming a CO_2 concentration of ~240 ppm. Yet, we believe that the intensity differences between the measured and predicted spectra are more likely due to our extension of the c-k model beyond its range

of validity. These relatively small differences in absolute intensities have little bearing on infrared signature masking issues.
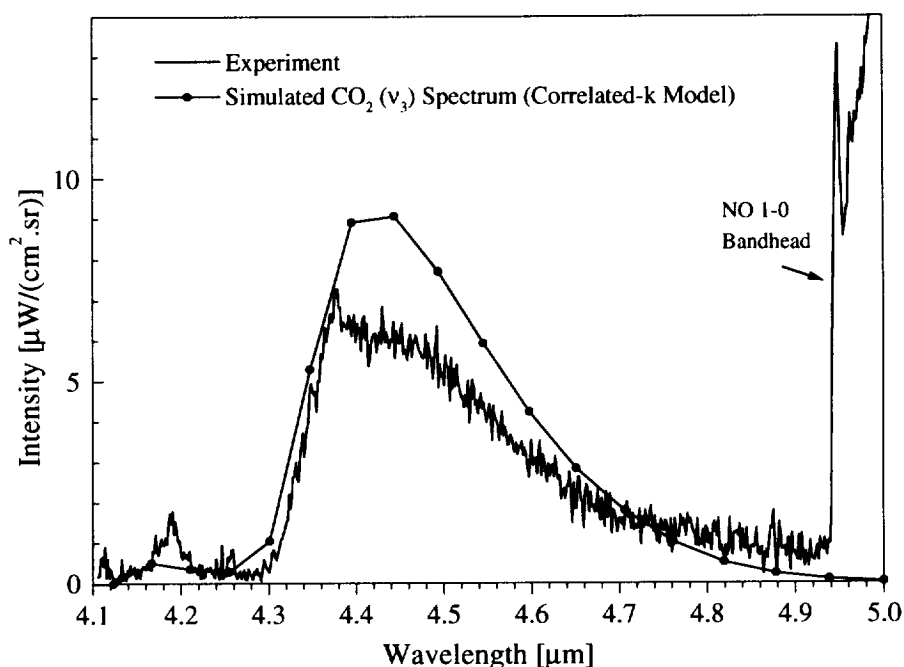

Figure 11. CO_2 spectrum computed with the c-k model parameters of the EM2C Laboratory,[6,7] and comparison with the measured spectrum. Note the effects of absorption by room air CO_2 in the range 4.2-4.4 μm.

4.3. Range 4.9- 5.6 μm

Figure 12 compares measurements and modeling results for NO fundamental bands. Two simulated spectra are presented, with and without incorporating the effects of water vapor absorption over the 6 meter path of room air between the plasma and the detector. By matching the depth of the water absorption features, we were able to determine the mole fraction of water vapor in the room to be approximately 0.014 (this value is slightly different from the 0.013 mole fraction used for the calibration recovery, because experiment and calibration were not conducted the same day). The room temperature and humidity were monitored (Oregon Scientific Instruments) during the scans of NO fundamental bands. The measured values of 25°C and 42% relative humidity correspond to a mole fraction of H_2O of 0.013 (Reynolds and Perkins,[13] p. 622), which is in excellent agreement with the mole fraction of 0.014 inferred from the absorption features of the measured spectrum.

As can be seen in Figure 12, the predictions of the model (with H_2O absorption) are in excellent agreement with the measured spectrum. It should be noted again that both the measurements and computations are on absolute intensity scales.
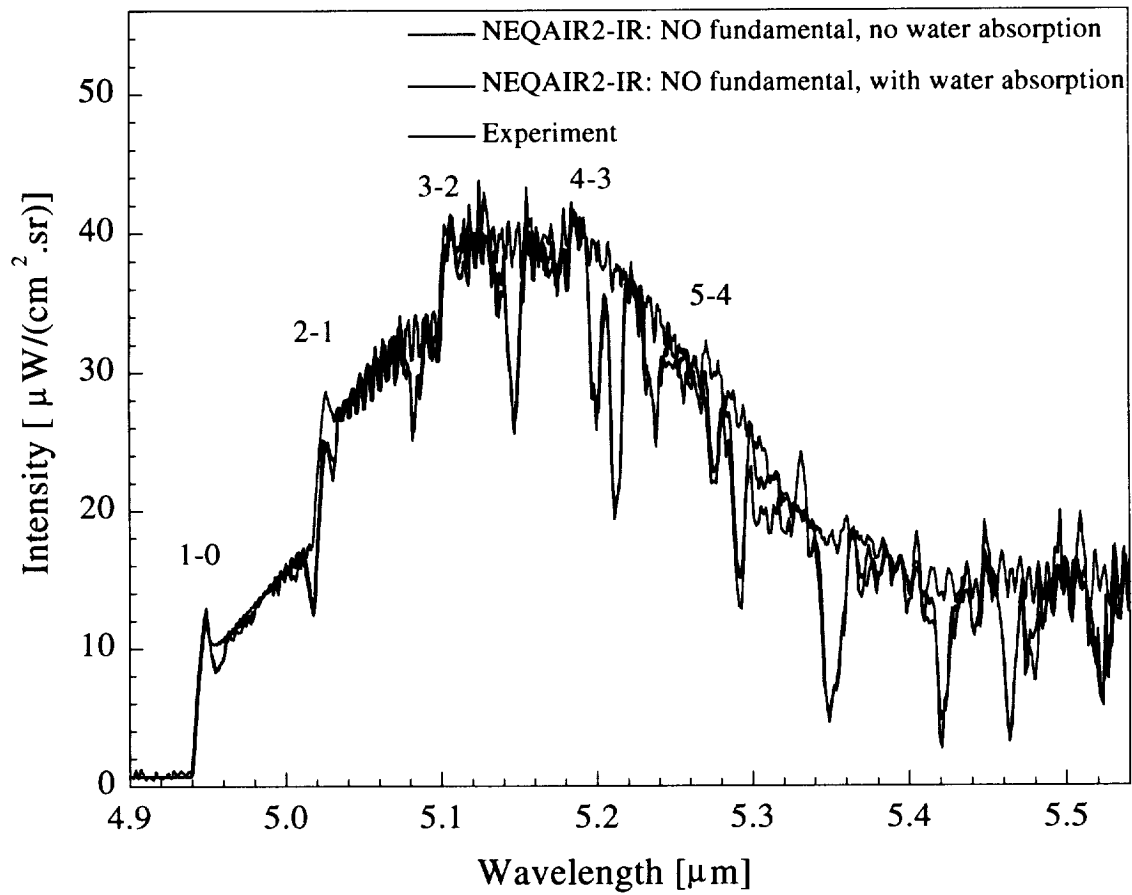
Figure 12. NO fundamental band spectrum computed with NEQAIR2-IR (with and without water vapor absorption), and comparison with experimental spectrum. Note that a (small) constant value of 0.8 $\mu W/(cm^2.sr)$ was added to the simulated spectra shown in the figure in order to match the offset, possibly due to underlying continuum radiation, that is apparent at 4.92 μm.

Summary and conclusions

Detailed measurements and modeling of the spectral emission of an atmospheric pressure air plasma at temperatures up to ~3400 K have been made. The cold gas injected in the plasma torch contained an estimated mole fraction of water vapor of approximately 4.5×10^{-3} and an estimated carbon dioxide mole fraction of approximately 3.3×10^{-4}. Under these conditions, the minimum level of air plasma emission is found to be between 3.9 and 4.15 μm. Outside this narrow region, significant spectral emission is detected that can be attributed to the fundamental and overtone bands of NO and OH, and to the v_3 and the (v_1+v_3) bands of CO_2. Special attention was paid to the effects of ambiant air absorption in the optical path between the plasma and the detector. Excellent quantitative agreement is obtained between the measured and simulated spectra, which are both on absolute intensity scales, thus lending confidence in the radiation models incorporated into NEQAIR2-IR over the course of this research program.

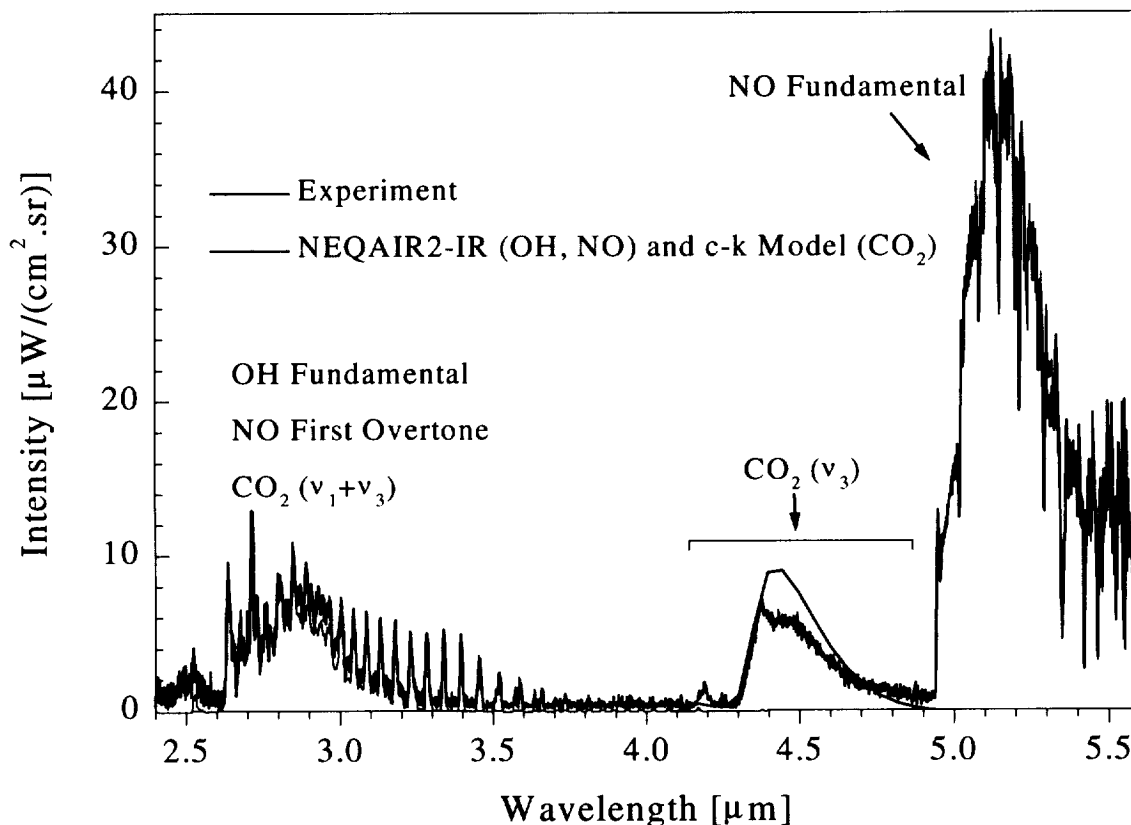Figure 13. Summary comparison between measurements and models of infrared emission by an air plasma at temperatures of ~3400 K and atmospheric pressure. The simulations incorporate the effect of water vapor and carbon dioxide absorption over the 6-meter length of room air between the plasma and the detector

5. Publications (June 1997- July 1998)

Levin, D.A., Laux, C.O, and Kruger, C.H., "A General Model for the Spectral Calculation of OH Radiation in the Ultraviolet," accepted for publication in *Journal of Quantitative Spectroscopy and Radiative Transfer,* February 1998.

Jenniskens, P, de Lignie, M., Betlem, H., Borovicka, J., Laux, C.O., Packan, D., and Kruger, C.H., "Preparing for the 1998/1999 Leonid Storms," subm. to *Icarus,* Nov. 1997.

Kruger, C.H., Owano, T.G., Laux, C.O., and Zare, R.N., "Nonequilibrium in Thermal Plasmas," *Journal de Physique IV,* Vol. 7, pp. C4-77–C4-92, October 1997.

Kruger, C.H., Owano, T.G., and Laux, C.O., "Experimental Investigations of Atmospheric Pressure Nonequilibrium Plasma Chemistry," Invited submission to the special issue "High Pressure Arcs and High Frequency Thermal Plasmas," *IEEE Transactions on Plasma Science,* Vol. 25, No. 5, pp. 1042-1051, October 1997.

Pierrot, L., Laux, C.O., and Kruger, C.H., "Consistent Calculation of Electron-Impact Electronic and Vibronic Rate Coefficients in Nitrogen Plasmas," 5th European Congress on Thermal Plasma Processes, Saint-Petersburg, Russia, July 13-16, 1998.

Pierrot, L., Laux, C.O., and Kruger, C.H., "Vibrationally-Specific Collisional-Radiative Model for Nonequilibrium Nitrogen Plasmas," *AIAA 98-2664,* 29th AIAA Plasmadynamics and Lasers Conference, Albuquerque, NM, June 15-18, 1998.

Nagulapally, M., Kolman, D., Candler, G.V., Laux, C.O., Gessman, R.J., and Kruger, C.H., "Numerical Simulation of a Nonequilibrium Air Plasma Experiment," 29th AIAA Plasmadynamics and Lasers Conference, Albuquerque, NM, June 15-18, 1998.

Laux, C.O., Gessman, R.J., Packan, D.M., Yu, L., Kruger, C.H., and R.N. Zare, "Experimental Investigations of Ionizational Nonequilibrium in Atmospheric Pressure Air Plasmas," 25th IEEE International Conference on Plasma Science (ICOPS), Raleigh, NC, June 1-4, 1998. (Invited)

Nagulapally, M., Kolman, D., Candler, G.V., Laux, C.O., Gessman, R.J., and Kruger, C.H., "Simulation of Nonequilibrium Plasma Experiments," 25th IEEE International Conference on Plasma Science (ICOPS), Raleigh, NC, June 1-4, 1998.

Schoenbach, K.H., Kunhardt, E.E., Laux, C.O., and Kruger, C.H., "Measurement of Electron Densities in Weakly Ionized Atmospheric Pressure Air," 25th IEEE International Conference on Plasma Science (ICOPS), Raleigh, NC, June 1-4, 1998.

Laux, C.O., Gessman, R.J., Owano, T.G., and Kruger, C.H., "Experimental Investigation of Nonequilibrium Plasma Chemistry at Atmospheric Pressure," presented at the 13th International Symposium on Plasma Chemistry, Beijing, China, August 18-22, 1997.

Owano, T.G., Laux, C.O., and Kruger, C.H., "Experimental Investigation of Nonequilibrium Plasma Chemistry at Atmospheric Pressure," Proceedings of the 13th

International Symposium on Plasma Chemistry, pp. 82-87, Beijing, China, August 18-22, 1997.

Kruger, C.H., Owano, T.G., Laux, C.O., and Zare, R.N., "Nonequilibrium in Thermal Plasmas," Proceedings of the 23rd International Conference on Phenomena in Ionized Gases, Toulouse, France, July 17-22, 1997 (invited). Also in *Journal de Physique IV*, Vol. 7, pp. C4-77–C4-92, October 1997.

Gessman, R.J., Laux, C.O., and Kruger, C.H., "Experimental Study of Kinetic Mechanisms of Recombining Atmospheric Pressure Air Plasmas," AIAA 97-2364, 28th AIAA Plasmadynamics and Lasers Conference, Atlanta, GA, June 23-25, 1997 (awarded best paper).

Candler, G.V., Laux, C.O., Gessman, R.J., and Kruger, C.H., "Numerical Simulation of a Nonequilibrium Nitrogen Plasma Experiment," AIAA 97-2365, 28th AIAA Plasmadynamics and Lasers Conference, Atlanta, GA, June 23-25, 1997.

Kruger, C.H., Owano, T.G., and Laux, C.O., "Diagnostics of Nonequilibrium Thermal Plasmas, with Applications to Diamond Synthesis," 23rd International Conference on Phenomena in Ionized Gases, Toulouse, France, July 17-22, 1997. (Invited)

Laux, C.O., Gessman, R.J., Hilbert, B., Packan, D.M., Pierrot, L.C., and Kruger, C.H., "Infrared Emission of Air Plasmas," Missile Signatures and Aerothermochemistry Meeting, Alexandria, VA, May 12-13, 1997.

6. Honors and Awards

June 1998: AIAA Plasmadynamics and Lasers Technical Committee Best Paper Award
Richard J. Gessman, Christophe O. Laux, and Charles H. Kruger, "Experimental Study of Kinetic Mechanisms of Recombining Atmospheric Pressure Air Plasmas," AIAA 97-2364, 28th AIAA Plasmadynamics and Lasers Conference, Atlanta, GA, June 23-25, 1997.

7. Personnel

The following personnel contributed to this report:
• Charles H. Kruger Professor, Vice-Provost, Dean of Research and Graduate Policy
• Christophe O. Laux, Research Associate
• Denis M. Packan, Graduate Research Assistant
• Richard J. Gessman, Graduate Research Assistant
• Laurent C. Pierrot, Postdoctoral Fellow

8. References

1. Laux, C.O., Gessman, R.J., Hilbert, B., and Kruger, C.H., "Experimental Study and Modeling of Infrared Air Plasma Radiation," *30th AIAA Thermophysics Conference, AIAA 95-2124*, San Diego, CA, 1995.

2. Amiot, C., "The Infrared Emission Spectrum of NO: Analysis of the $\Delta v=3$ sequence up to $v=22$," *Journal of Molecular Spectroscopy*, **94**, 150, 1982.

3. Langhoff, S.R. and Bauschlicher, C.W., Jr, "Theoretical Dipole Moment for the $X^2\Pi$ state of NO," *Chem. Phys. Letters*, **223**, 416-422, 1994.

4. Spencer, M.N., Chackerian, C., Jr., and Giver, L.P., "The Nitric Oxide Fundamental Band: Frequency and Shape Parameters for Rovibrational Lines," *J. Molec. Spectrosc.*, **165**, 506-524, 1994.

5. Goody, R. and Young, Y., *Atmospheric Radiation,*, 2nd ed. Oxford, 1989.

6. Soufiani, A. and Taine, J., "High Temperature Gas Radiative Property Parameters of Statistical Narrow-band Models for H_2O, CO_2, and CO and correlated-k Model for H_2O and CO_2," *Int. Journal of Heat and Mass Transfer*, **40**, 987-991, 1997.

7. Pierrot, L., "Développement, étude critique et validation de modèles de propriétés radiatives infrarouges de CO_2 et H_2O à haute température. Application au calcul des transferts dans des chambres aéronautiques et à la télédétection," Thesis, Ecole Centrale Paris, 1997.

8. Stark, G., Brault, J.W., and Abrams, M.C., "Fourier-Transform Spectra of the $A^2\Sigma^+$-$X^2\Pi$ $\Delta v = 0$ Bands of OH and OD," *J. Opt. Soc. Am. B*, **11**, 3-32, 1994.

9. Levin, D.A., Laux, C.O., and Kruger, C.H., "A General Model for the Spectral Radiation Calculation of OH in the Ultraviolet," *accepted for publication in JQSRT*, 1998.

10. Coxon, J.A., "Optimum Molecular Constants and Term Values for the $X^2\Pi$ ($v \le 5$) and $A^2\Sigma^+$ ($v \le 3$) States of OH," *Can. J. Phys.*, **58**, 933-949, 1980.

11. Holtzclaw, K.W., Person, J.C., and Green, B.D., "Einstein Coefficients for Emission from High Rotational States of the OH ($X\ ^2\Pi$) Radical," *JQSRT*, **49**, 223-235, 1993.

12. Rothman, L.S., Gamache, R.R., Tipping, R.H., Rinsland, C.P., Smith, M.A.H., Chris Benner, D., Malathy Devi, V., Flaud, J.-M., Camy-Peyret, C., Perrin, A., Goldman, A., Massie, S., Brown, L.R., and Toth, R.A., "The HITRAN Molecular Database: Editions of 1991 and 1992," *JQSRT*, **48**, 469-507, 1992.

13. Reynolds, W.C. and Perkins, H.C., *Engineering Thermodynamics*, Mc Graw Hill, New York, 1977.